Thermal Stress Analysis of Parabolic Trough Receivers with Concentrated Solar Radiation

Dongqiang Lei[1,2,3,4] Xuqiang Fu[5] Yucong Ren[1,2,3] Zhifeng Wang[1,2,3,4]

[1]Key Laboratory of Solar Thermal Energy and Photovoltaic System, Institute of Electrical Engineering, Chinese Academy of Sciences;

No.6 Beiertiao, Zhongguancun, Beijing, China, 100190.

[2]Beijing Engineering Research Center of Solar Thermal Power;

No.6 Beiertiao, Zhongguancun, Beijing, China, 100190.

[3]University of Chinese Academy of Sciences;

No.19 (A) Yuquan Rd, Shijingshan District, Beijing, P.R.China 100049

[4]China National Solar Thermal Energy Alliance;

No.6 Beiertiao, Zhongguancun, Beijing, China, 100190.

[5]Hebei University of Technology, Xiping Road No. 5340, Beichen District, Tianjin, China,300130.

Abstract

The failure of receiver tube is the primary ongoing issue in the parabolic trough power system. In this study, the stress field of the receiver is studied by numerical simulation and the field measurements. The three-dimensional numerical simulation on the whole receiver is conducted firstly by combining the Monte-Carlo Ray Tracing method and the Finite Volume Method. The temperature, the heat loss and the expansion length of the receiver were tested on a heat loss test bench. The simulated concentrated heat flux on the absorber tube and the glass envelope have good agreement with Jeter's results. The temperature field of the entire receiver then was used to analyze the thermal stress and the deformation of the receiver. Finally, the effects of the DNI, the fluid temperature and flow rate on the temperature gradients and the thermal stress fields of the whole receiver were studied. The absorber tube bending and glass to metal seals failure were also analyzed. The Von-Misses stress and allowable strain of 316L stainless steel were used to analyze the deformation and the fatigue failure of the receiver.

Keywords: parabolic trough receiver, thermal stress, DNI, temperature distribution

1. Introduction

Solar thermal electricity generation is one of the feasible renewable technologies to reduce the consumption of conventional fossil fuels and CO_2 emissions. At present, large-scale solar thermal electricity generation mainly has four types of systems: parabolic trough, solar tower, solar dish and linear Fresnel, among them parabolic trough technology is the most proven and widespread solar thermal power technology today.

In a parabolic trough system, the mirrors concentrate the sun rays on the receivers. The heat transfer fluid (HTF) passes through the receivers and transfers heat from the receiver tubes to a heat exchanger in a power station. The receiver is one of the most important elements in the system for converting the solar energy into thermal energy of HTF. The parabolic trough receiver consists of an absorber tube with a selective coating and a glass envelope surrounding the absorber tube to form a vacuum annular space between the glass envelope and the absorber tube. A glass to metal sealing element is arranged on each free end of the glass envelope, wherein the central absorber tube and the glass to metal sealing element are connected with each other by means of bellows, as shown in Fig. 1 (Price et al. 2002). In order to decrease the sealing residual stress, a thermal coefficient matched material combination that composed of the Kovar alloy and the 5.0 borosilicate glass was applied in the receiver studied in this paper (Lei et al. 2012).

doi:10.18086/swc.2017.04.08 Available at http://proceedings.ises.org

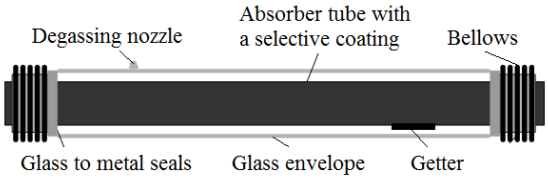

Fig.1 Typical parabolic trough receiver

The receiver's structural reliability has a significant influence on the safety and economic operation of the parabolic trough system (Cheng et. 2010, Glenn, 2012). Data from existing commercial parabolic trough power stations show that receiver failure is the primary ongoing issue. The first nine solar energy generation system plants (SEGS) have experienced very high receiver failure (about 5.5% per year) in the first few years (Price, 2002,). The most recent data for SEGS pants indicated that receiver failures had decreased to 3.4% of the total field receivers per year, which still seems unacceptably high. These failures involved vacuum loss, glass envelope breakage and degradation of the coating. Of these failures, 55% were reported to involve broken glass and 29% involved loss of vacuum, in most cases due to the failure of glass to metal seals, but also due to bowing tubes (Mills, 2004). The receivers themselves represent 30% of the solar field material cost and would require additional labor to replace (Charles, 2010).

In order to investigate the failure mechanisms, some researchers have focused on the temperature gradients and stress fields on the absorber tube due to the non-uniform heat flux (Cheng et al. 2010; Wu et al. 2014b; Abedini et al. 2015). The literature survey shows that most of their models mentioned above ignored the end parts of the receiver (without bellows and glass to metal sealing element). There are few researchers to study the detailed heat transfer and thermal stress of whole receiver under non-uniform concentrated solar heat flux in a parabolic trough system. They did not consider the temperature and stress distribution of the bellows and the glass to metal seals which could result in the glass envelope breakage or vacuum loss. Especially, their models ignored the effect of the bellows and glass envelope on the temperature and stress distribution of the absorber tube. Actually, the bellows and glass envelope will also affect or constrain the axial expansion of the absorber tube.

In this paper, the stress distribution of the whole receiver is further studied by numerical simulation and the experimental measurements. The three-dimensional numerical simulation on the whole receiver is conducted firstly by combining the MCRT method and the FVM. The non-uniform concentrated heat flux on the absorber tube and the glass envelope was obtained through the coordinate transformations (CT) and Monte-Carlo ray tracing (MCRT) method. The heat flux verified by comparing with Jeter's results was used as a boundary condition of the coupled heat transfer modeling. The processes of fluid dynamics and coupled heat transfer of the receiver was analyzed by FVM. Then the temperature, the heat loss and the expansion length of the receiver were tested on a heat loss test stand. After validation, the temperature field of the entire receiver was used to analyze the thermal stress and the deformation of the receiver. Finally, the effects of the DNI, the fluid temperature and flow rate on the temperature gradients and the thermal stress fields of the whole receiver were studied. The absorber tube bending and glass to metal seals failure were also analyzed. The Von-Misses stress and allowable strain of 316L stainless steel were used to analyze the deformation and the fatigue failure of the receiver.

2. Methodology

There are three steps for the methodology in this study. Firstly, the solar energy flux distribution on the selective coating and glass envelope is calculated and validated. Secondly, three dimensional temperature distribution of the whole parabolic trough receiver tube is analyzed based on the previous step as a boundary condition. At the third step, the temperature distribution data are used to calculate the thermal stress and deformation of the receiver tube.

2.1. Simulation of solar energy flux distribution

The coordinate transformations (CT) and Monte-Carlo ray tracing (MCRT) method were combined to simulate the solar energy flux distribution on the receiver tube. In the simulation process, non-parallelism of solar rays with a 9.3mrad optics cone, rim angle, transmittance of the glass tube, absorptance of the coating, reflectance of the glass tube and reflectance of the parabolic trough mirror were considered (Zhao et al. 2015). The detail calculating process was presented in the Ref. Zhao et al. 2015. The heat distributions on the selective coating and the glass tube were calculated under the same parameters as Jeter’s (Jeter, 1986). The simulation results in this paper show that the heat flux distribution has a very good agreement with Jeter’s results as shown in Fig.2. The heat flux on the absorber tube is low near angle of 0 °due to the radiation shadow of the absorber, and then increases very fast up to

the maximum value. After that, the heat flux decreases down rapidly with the angel and then it keeps the minimum value due to the one sun radiation. The heat flux distributions on absorber tube and glass envelope were treated as the heat flux boundary for the heat transfer simulation model.

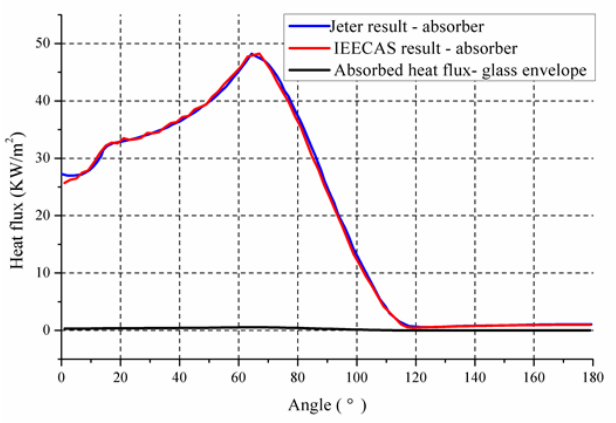

Fig. 2 Simulated heat flux distribution result compared with Jeter's result

2.2. Simulation of temperature distribution

In typical parabolic trough solar system, the solar radiation is reflected and concentrated on the glass envelope, and then it transmits the glass envelope and finally arrives on the coating of the absorber tube. The coating converts the solar energy into the heat energy, and then the heat energy is conducted to the absorber inner surface. The heat transfer fluid (HTF) passes through the absorber tube then obtains the heat energy by convection. Meanwhile, a part of heat energy (heat loss) passes through the glass thickness and by radiation and convection to the environment from the outer surface of the glass envelope.

2.2.1 Assumptions in the simulation

A three-dimensional computational fluid dynamics and heat transfer simulation of whole receiver was established. Fig. 3 shows the three dimensional mesh of the receiver tube used in this study. All of the meshes were generated with O-grid method by Ansys ICEM. After performing a grid independent, the study based on the variation of frictional pressure drop and temperature increase within the absorber tube, a grid of 3,000,000 cells was chosen for the simulation of the temperature and the stress distribution.

In order to investigate the temperature gradient in the glass-to-metal seals and the bellows, finer grids were generated near the glass-to-metal seals where large temperature gradient exists.

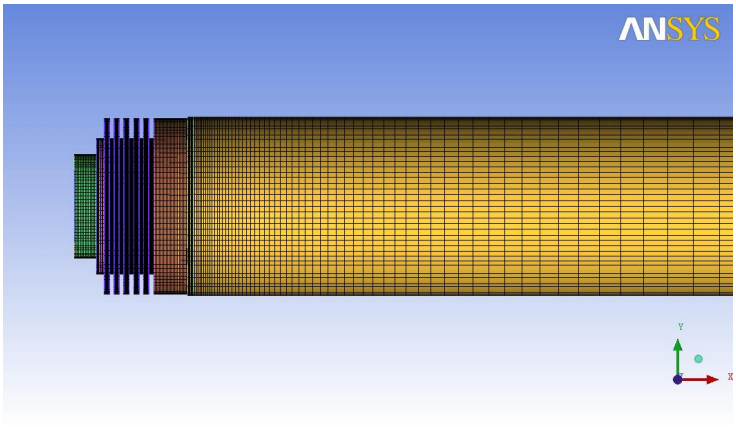

Fig. 3 Three-dimensional mesh of the receiver tube

The three dimensional heat transfer problem was solved using FVM model. Some assumptions in the simulation are listed as follow:

1) The vacuum level between the absorber tube and the glass envelope is so good that the convection can be ignored.

2) The fluid flow is in steady state conditions. The calculated Reynolds number ($Re=\rho ud/\mu$) of HTF flow in the absorber tube is much higher than 2300, and the flow is turbulent. Therefore, standard k-ε model, a turbulence model, was used in this study.

2.2.2 The governing equations

The governing equations include continuity equation, momentum equation, energy equation and standard k-ε two-equation turbulence model equation.

Continuity equation:

$$\frac{\partial}{\partial X_i}(\rho U_i) = 0 \quad \text{(eq.1)}$$

Momentum equation:

$$\frac{\partial p}{\partial x_i} = \rho g_i + \frac{\partial}{\partial x_j}[(\mu+\mu_t)(\frac{\partial u_i}{\partial x_j}+\frac{\partial u_j}{\partial x_i}) - \frac{2}{3}(\mu+\mu_t)\frac{\partial u_l}{\partial x_l}\delta_{ij}] - \frac{\partial}{\partial x_i}(\rho u_i u_j) \quad \text{(eq.2)}$$

Energy equation:

$$\frac{\partial}{\partial x_i}(\rho c_p u_i T) = -\lambda\frac{\partial T}{\partial x_i} \quad \text{(eq.3)}$$

κ equation:

$$\frac{\partial(\rho u_i \kappa)}{\partial x_i} = G_k - \rho\varepsilon + \frac{\partial}{\partial x_i}[(\mu+\frac{\mu_t}{\sigma_k})\frac{\partial \kappa}{\partial x_i}] \quad \text{(eq.4)}$$

ε equation:

$$\frac{\partial(\rho u_i \varepsilon)}{\partial x_i} = C_1 G_k\frac{\varepsilon}{\kappa} - C_2\rho\frac{\varepsilon^2}{\kappa} + \frac{\partial}{\partial x_i}[(\mu+\frac{\mu_t}{\sigma_\varepsilon})\frac{\partial \varepsilon}{\partial x_i}] \quad \text{(eq.5)}$$

With

$$\mu_t = C_\mu\rho\frac{\kappa^2}{\varepsilon}, \quad G_k = \mu_t\frac{\partial u_i}{\partial x_j}(\frac{\partial u_i}{\partial x_j}+\frac{\partial u_j}{\partial x_i}) \quad \text{(eq.6)}$$

The model constants $C_1, C_2, C_\mu, \sigma_\kappa, \sigma_\varepsilon$ have the following default values:

$$C_1 = 1.44, C_2 = 1.92, C_\mu = 0.09, \sigma_K = 1, \sigma_\varepsilon = 1.3$$

2.2.3 Boundary conditions

(1) The following boundary conditions are applied to the inlet and outlet:

Inlet: $u_x = u_{in}, u_y = u_z = 0, T = T_{in}$

$\kappa_{in} = 0.005u_x^2, \varepsilon_{in} = c_\mu \cdot \rho(T)\cdot\kappa_{in}^2/\mu_t$, where $c_\mu = 0.09, \mu_t = 100$

Outlet: fully-developed conditions.

(2) The selective coating is defined as a wall with the heat flux distribution calculated by the CT and MCRT Method.

(3) Surface-to-surface (S2S) radiation model is used between the selective coating and inner surfaces of the glass envelope, the Kovar rings and the bellows. The participating surfaces were assumed to be gray and diffuse.

(4) The outer surface of the glass envelope was defined with the equivalent coefficient of convective heat transfer for convection and radiation.

2.3. Simulation of thermal stress

The ANSYS software was used in the thermal stress analysis. Except the temperature distribution data of HTF, the temperature distribution data of the receiver obtained in the CFD analysis were imported into the nodes of thermal-stress analysis model with the same grids as the temperature analysis model. According to the materials used in the receiver, thermo-elastic equations of hollow cylinder were solved by using finite element analysis (FEA) with the aim of calculating thermal stress field and deformation for the receiver in this study.

In the parabolic trough collectors, the receiver tubes of the triples are generally straight and the mounting arms can compensate the axial heat expansion of the absorber tubes. In the study, one end of the absorber tube was fixed in X axial direction however the other end was allowed to move along the X axis freely and rotate around the X axis freely. The gravity of the receiver tube was considered and its direction was assumed the negative Z axial direction.

In the parabolic trough receiver, although the bellows are used to compensate the axial and radial expansion differences between the glass envelope and the absorber tube, the bellows are mainly subject to the axial force and affect the deformation of the absorber tube in actual operation. Therefore, the bellows axial stiffness was considered and input into the Ansys software.

In this study, the analysis of thermal stress field considers the combined effects of temperature gradients, support constraints, internal constraints and gravity. According to the Von-Mises theory, the equivalent stress equation is expressed as follows:

$$\sigma_{eff} = \sqrt{\sigma_x^2 + \sigma_y^2 + \sigma_z^2 - (\sigma_x\sigma_y + \sigma_x\sigma_z + \sigma_z\sigma_y)} \quad \text{(eq.7)}$$

The Von-Misses stress and allowable strain of 316L stainless steel were used to analyzed the deformation and the failure of the receiver

3. Experimental system description

A heat loss test stand was built in Institute of Electrical Engineering, Chinese Academy of Sciences (IEECAS). This test bench was used to test the temperature of the glass envelope and the heat loss of the receiver. In order to get the real thermal emittance of the coating, the heat losses depended on temperature were used to calculate the thermal emittance (Lei et al. 2013).

Fig. 3 Receiver heat loss test stand at IEECAS

4. Results and discussion

4.1. Validations of numerical simulation results

4.1.1 Comparison between FVM model and experiment

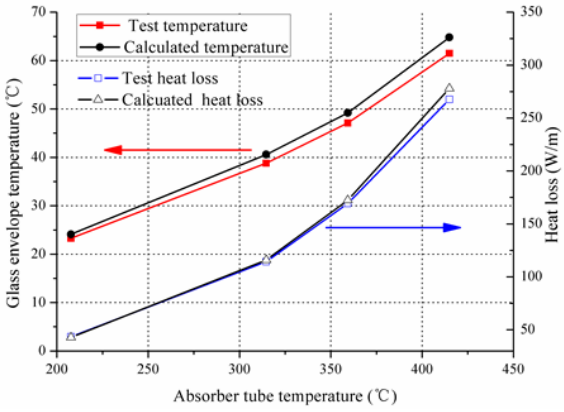

Fig. 4 Compared results between the test and the simulation

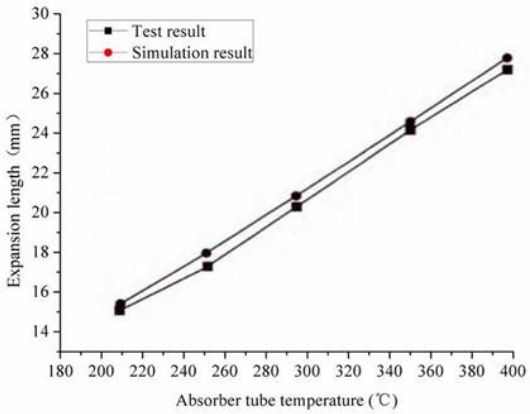

Fig. 5 Simulated result compared with test result

The FVM model generally can be validated by comparing the heat loss test results (Wu et al. 2014a; Chenget al. 2010). A heat loss test bench of the receiver was built in IEECAS in 2012. The heat loss test method, procedure, test conditions and results were described in Ref.12 in detail. In this paper, the same test conditions as the Ref.12 were used to calculate the temperature and the heat loss of the receiver. In the simulation, the inner surface temperature of the absorber tube was assumed to be constant, and no HTF was in the absorber tube. The average temperature of the glass envelope was calculated by the same method in the heat loss test. The heat loss was obtained by calculating the heat flux from the inner surface of the absorber tube in the simulation. Fig. 4 shows the compared results between the test and the simulation. The heat loss difference between the simulation results and the test results were between 1.6 and 10.3W/m with a relative error range of 1.4%-3.8%. The calculated glass envelope temperature had a maximum 5.4% relative error with the test results. Considering the uncertainty associated in both simulation and test, the agreement is very good. The uncertainty in the simulation contains the uncertainty of the equivalent convective heat transfer coefficient used between the glass envelope and the ambient and the thermal emittance of the coating. Especially, the thermal emittance of the coating is a very important parameter for the simulation and can remarkably affect the simulated results. If the thermal emittance increases only 1%, the heat loss will increase about 10%. Therefore, the thermal emittance of the coating should be tested at different temperature because it is temperature-dependent. In this paper, the thermal emittance of the coating has been tested in IEECAS heat loss test bench. Therefore, the numerical simulation methodology is valid in this study.

4.1.2 Comparison between FEA model and experiment

The validation of FEA model with real field test results is very difficult because the complicated external environment, such as the real concentrated heat flux, the changeable wind speed, the installation error, the end support condition of the receiver and the mirror shape error. In addition, the internal mechanical stress and residual stress on the receiver tube also affect the test results.

Fig. 5 indicates the expansion length curves of the absorber tube with temperature. The expansion length of the absorber tube was tested when the heat loss test was carried out. It shows that the simulation results agree with the test results very well. The maximum HTF temperature is generally less than 400℃ in parabolic trough system, the material of the absorber tube is within the elastic range. Therefore, if the two end supports do not constrain the axial expansion of the absorber tube, the stress is caused only by temperature and is linear functional relation with the thermal strain in the absorber tube. The FEA methodology is valid and reliable for the stress analysis on the absorber tube.

4.2. Temperature distribution of receiver tube

In order to calculate thermal stress field, the temperature distributions of the whole receiver and the key components were shown in Fig.6.

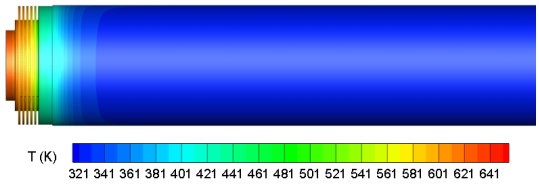

Fig.6 Temperature distributions of the whole receiver tube and the key components

In Fig. 6, DNI is 1000W/m^2. HTF inlet temperature is 350℃ and the flow rate is 2 m/s which is a typical condition in system operation. Fig.10 a) shows the temperature distribution on the out surface of the whole receiver tube. The temperature varies considerably at the end of the receiver tube, which decreases from 641K to 321K from the end of the absorber to the middle of the glass envelope. Therefore, the receiver is subject to very large temperature gradients in operation. In order to obtain the temperature information of the key components in detail, Fig. 6 clearly exhibits the temperature distribution of the absorber tube, the Kovar ring and the bellows. It shows that the temperature distribution is very nonuniform along both the axial and the circumferential direction of the absorber tube. The larger temperature gradient occurred on the end part of the absorber tube due to the shield of the bellows and the glass to metal sealing element. This nonuniform temperature along the axial direction of the absorber tube can also cause thermal stress and the deformation of the absorber tube. Therefore, it is not reasonable to ignore the bellows and the glass metal sealing elements when the temperature and stress are simulated for the receiver. The temperature distribution of cross section of the absorber tube and HTF is symmetrical approximately, which is very similar to the heat flux distribution on the surface (see Fig. 2). This temperature difference creates variable expansion and nonuniform deformation of the absorber tube. The above temperature data are very important and helpful for the structure design, optimization and the reliable operation of the receiver.

4.3. Stress distribution and deformation of receiver tube

The temperature information was further used to analyze the thermal stress distribution on the whole receiver tube. Fig. 7 shows the stress distributions on the absorber tube, the glass envelope, the bellows and the Kovar ring. The stress distribution on the absorber tube is nonuniform and similar to the temperature distribution and the heat flux distribution. The maximum equivalent tensile stress is a bout 34MPa at the place of the maximum heat flux density. It also shows that the absorber tube has a little deflection of 4.2mm, as shown in Fig 7 a). In the field test, although the absorber bending has been seen, the deflections of the absorber tubes are no any rule when HTF velocity is higher than 1m/s. When HTF velocity is lower than 1m/s, the absorber tube can easily bend and the bending generally is permanent. The absorber tube bending can cause part of solar radiation out of the absorber tube and decreases the thermal efficiency of the collector.

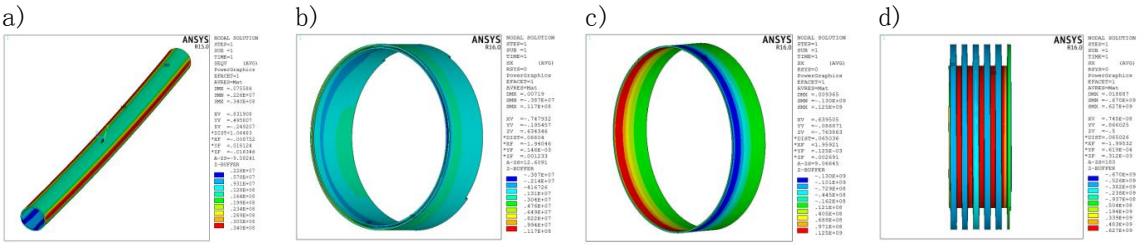

Fig. 7 stress distributions on the absorber tube, the glass envelope, the bellows and the Kovar ring

Fig. 7 b) and c) illustrate the axial stress distribution on the end of glass envelope and the Kovar ring. The two figures present that the bigger stress concentration occurs at the junction between the Kovar ring and the glass envelope. The maximum tensile stress of 11MPa locates at the end of the glass envelope. The reason may be that the expansion difference between the absorber tube and the glass envelope causes the tensile force on the end of the glass envelope, and the expansion difference between the Kovar ring and the glass also causes the tensile stress on the end of the glass envelope. If the coefficient of thermal expansion (CTE) of the Kovar ring is much bigger than CTE of the glass envelope, the larger tensile stress may exceed the tensile strength of the glass and cause the glass break. Therefore, the difference of CTEs between the glass and the metal is an important factor affecting the magnitude of stress.

The stress distributions on the bellows are also very nonuniform, as shown in Fig.7 d). The maximum axial stress is at the third trough of the bellows. The bellows are subject to the larger axial stress due to the expansion difference between the glass envelope and the absorber tube. While the maximum equivalent stress of 757 MPa is at the wield

junction between the bellows and the Kovar ring, which the magnitude may be too big. The authors contribute the large equivalent stress to the difference of CTEs between the Kovar ring and the bellows, and the unsuitable elastic modulus or axial stiffness used in simulation. Because the thickness of the bellows is generally 0.2-0.3mm and the bellows cyclically expand and compress every day, the bellows with large stress are easy to fatigue or crack, and then lead to the vacuum failure of the receiver. Therefore, the bellows, as the key component, should have enough fatigue strength and be protected from any concentrated solar radiation.

5. Conclusions

In this study, the distributions of the temperature and the stress were studied by numerical simulation and the experimental measurements. The three-dimensional numerical simulation on the whole receiver was conducted successfully by combining the MCRT method, the FVM and the FEA. The distributions of the temperature and the stress were analyzed for the whole receiver including the bellows, the Kovar ring, the glass envelope and the absorber tube in detail. After validating the numerical model, the effects of the fluid temperature and flow rate on the temperature gradients and the thermal stress fields of the whole receiver were studied. The results show that：

1） Thermal emittance of the coating should be tested at different temperature because it is a very important parameter in the simulation and can remarkably affect the simulated temperature results.

2） The stress distribution is nonuniform along both the axial and the circumferential direction on the absorber tube, which is similar to the temperature distribution and the solar flux distribution.

3） The bigger stress concentration occurs at the junction between the Kovar ring and the glass envelope. The difference of CTEs between the glass and the metal is an important factor affecting the magnitude of stress.

4） The bellows are subject to the larger axial stress due to the expansion difference between the glass envelope and the absorber tube.

6. Acknowledgements

The authors thank Ph. D Zhiyong Wu for his technical assistance of CFD software. This study was supported by the National Nature Science Foundation of China (Grant No. 51476165).

7. References

Abedini-Sanigy, M. H., et al. (2015). Thermal Stress Analysis of Absorber Tube for a Parabolic Collector under Quasi-Steady State Condition. Energy Procedia 69(0): 3-13.

Charles MM, Craig T, Glatzmaier G, 2010. Line-Focus Solar Power Plant Cost Reduction Plan, National Renewable Energy Laboratory NREL/TP-5500-48175.

Cheng ZD, He YL, Xiao J, Tao YB, 2010. Three-dimensional numerical study of heat transfer characteristics in the receiver tube of parabolic trough solar collector, International Communications in Heat and Mass Transfer, 37 (2010) 782–787

Glenn KW, Ho CK, 2012. Impact of Aperture Size, Receiver Diameter, and Loop Length on Parabolic Trough Performance with Consideration of Heat Loss, Pumping Parasitics, and Optics for a Typical Meteorological Year. SolarPACES 2012, Marrakech, Morocco, September 11-14.

Jeter SM, 1986. Calculation of the concentrated flux density distribution in parabolic trough collectors by a semifinite formulation, solar energy vol. 37, no. 5, pp. 335-345.

Lei, D. Q., et al. (2010). The calculation and analysis of glass-to-metal sealing stress in solar absorber tube. Renewable Energy 35(2): 405-411.

Lei, D., et al. (2012). Experimental study of glass to metal seals for parabolic trough receivers. Renewable Energy 48(0): 85-91.

Lei, D., et al. (2013). An experimental study of thermal characterization of parabolic trough receivers. Energy Conversion and Management 69(0): 107-115.

Mills, D. (2004). Advances in solar thermal electricity technology. Solar Energy 76(1-3): 19-31.

Price, H., et al. (2002). Advances in Parabolic Trough Solar Power Technology. Journal of Solar Energy

Engineering 124(2): 109-125.

Wu, Z., et al. (2014a). Structural reliability analysis of parabolic trough receivers. Applied Energy 123(0): 232-241.

Wu, Z., et al. (2014b). Three-dimensional numerical study of heat transfer characteristics of parabolic trough receiver. Applied Energy 113: 902-911.

Zhao, D., et al. (2015). The Simulation Model of Flux Density Distribution on an Absorber Tube. Energy Procedia 69: 250-258.